

This discussion paper is/has been under review for the journal Atmospheric Measurement Techniques (AMT). Please refer to the corresponding final paper in AMT if available.

Evaluation of the Airborne Quantum Cascade Laser Spectrometer (QCLS) measurements of the carbon and greenhouse gas suite – CO₂, CH₄, N₂O, and CO – during the CalNex and HIPPO campaigns

G. W. Santoni¹, B. C. Daube¹, E. A. Kort², R. Jiménez³, S. Park⁴, J. V. Pittman¹, E. Gottlieb¹, B. Xiang¹, M. S. Zahniser⁵, D. D. Nelson⁵, J. B. McManus⁵, J. Peischl^{6,7}, T. B. Ryerson⁷, J. S. Holloway⁷, A. E. Andrews⁷, C. Sweeney⁶, B. D. Hall⁷, E. J. Hintsa^{6,7}, F. L. Moore^{6,7}, J. W. Elkins⁷, D. F. Hurst^{6,7}, B. B. Stephens⁸, J. D. Bent⁹, and S. C. Wofsy¹

¹Harvard University, School of Engineering and Applied Sciences and Department of Earth and Planetary Sciences, Cambridge, Massachusetts, USA

²Jet Propulsion Laboratory, California Institute of Technology, Pasadena, California, USA

³University of Colombia, Chemical Engineering and Environmental Studies, Bogota, Colombia

Evaluation of the Airborne Quantum Cascade Laser Spectrometer (QCLS)

G. W. Santoni et al.

Title Page

Abstract

Introduction

Conclusions

References

Tables

Figures

⏪

⏩

◀

▶

Back

Close

Full Screen / Esc

Printer-friendly Version

Interactive Discussion



⁴Department of Oceanography, College of Ecology and Environmental Science, Kyungpook National University, Republic of Korea

⁵Aerodyne Research, Inc., Center for Atmospheric and Environmental Chemistry, Billerica, MA, USA

⁶Cooperative Institute for Research in Environmental Sciences, University of Colorado, Boulder, Colorado, USA

⁷Earth System Research Laboratory, National Ocean and Atmospheric Administration, Boulder, Colorado, USA

⁸National Center for Atmospheric Research, Earth Observing Laboratory, Boulder, Colorado, USA

⁹Scripps Institution of Oceanography, La Jolla, California, USA

Received: 7 October 2013 – Accepted: 14 October 2013 – Published: 13 November 2013

Correspondence to: G. W. Santoni (gsantoni@gmail.com)

Published by Copernicus Publications on behalf of the European Geosciences Union.

Evaluation of the Airborne Quantum Cascade Laser Spectrometer (QCLS)

G. W. Santoni et al.

Title Page

Abstract

Introduction

Conclusions

References

Tables

Figures

⏪

⏩

◀

▶

Back

Close

Full Screen / Esc

Printer-friendly Version

Interactive Discussion

Abstract

We present an evaluation of aircraft observations of the carbon and greenhouse gases (CO₂, CH₄, N₂O, and CO) using a direct-absorption pulsed quantum cascade laser spectrometer (QCLS) operated during the HIPPO and CalNex airborne experiments.

5 The QCLS made continuous 1 Hz measurements with 1-sigma Allan precisions of 20, 0.5, 0.09, and 0.15 ppb for CO₂, CH₄, N₂O, and CO, respectively, over > 500 flight hours on 79 research flights. The QCLS measurements are compared to two vacuum ultraviolet (VUV) CO instruments (CalNex and HIPPO), a cavity ring-down spectrometer (CRDS) measuring CO₂ and CH₄ (CalNex), two broadband non-dispersive infrared spectrometers (NDIR) measuring CO₂ (HIPPO), two onboard gas chromatographs measuring a variety of chemical species including CH₄, N₂O, and CO (HIPPO), and various flask-based measurements of all four species. QCLS measurements are tied to NOAA and WMO standards using an in-flight calibration system and mean differences when compared to NOAA CCG flask data over the 59 HIPPO research flights were 100, 1, 1, and 2 ppb for CO₂, CH₄, N₂O, and CO, respectively. The details of the end-to-end calibration procedures and the data quality-assurance and quality-control (QA/QC) are presented. Specifically, we discuss our practices for the traceability of standards given uncertainties in calibration cylinders, isotopic and surface effects for the long-lived greenhouse gas tracers, interpolation techniques for in-flight calibrations, and the effects of instrument linearity on retrieved mole fractions.

1 Introduction

Growing interest in understanding the drivers of climate change has sparked innovation in instrumentation to measure long-lived greenhouse gases and associated chemical tracers (Chen et al., 2010; Fried et al., 2009; Nelson et al., 2004; O'Shea et al., 2013; Xiang et al., 2013a; Zare et al., 2009). The improvements in measurement precision and ease-of-use must be matched with a corresponding increase in calibration

AMTD

6, 9689–9734, 2013

Evaluation of the Airborne Quantum Cascade Laser Spectrometer (QCLS)

G. W. Santoni et al.

Title Page

Abstract

Introduction

Conclusions

References

Tables

Figures

⏪

⏩

◀

▶

Back

Close

Full Screen / Esc

Printer-friendly Version

Interactive Discussion

Evaluation of the Airborne Quantum Cascade Laser Spectrometer (QCLS)

G. W. Santoni et al.

Title Page

Abstract

Introduction

Conclusions

References

Tables

Figures

⏪

⏩

◀

▶

Back

Close

Full Screen / Esc

Printer-friendly Version

Interactive Discussion

efforts to achieve comparable gains in compatibility. Many sensors rely on the accuracy of spectroscopic parameters (e.g., line strengths and their pressure and temperature dependencies) to derive in situ “spectroscopically-calibrated” mixing ratios from raw spectra (Rothman et al., 2009; Zahniser et al., 1995). The use of this raw data is often appropriate, particularly if: (1) a sensor is linear with respect to the range of observed concentrations, and (2) the quantity of interest is the relative enhancement of one chemical tracer vs. another or vs. background values measured on the same sensor. More and more studies, however, are incorporating data from different sensors (Gerbig et al., 2003; Zhao et al., 2009; Xiang et al., 2013b; Miller et al., 2008). It is in this context that spectroscopically-calibrated mixing ratios are insufficient, as small differences in sensor accuracies can have large effects, e.g., on inversion studies.

Here we discuss the traceability of airborne in situ spectrometer measurements. We present an overview of the quantum cascade laser spectrometer (QCLS) sensor used on two airborne campaigns—the HIAPER Pole-to-Pole Observations (HIPPO; Wofsy et al., 2011) campaign on the NCAR HIAPER-GV and the California Research at the Nexus of Air Quality and Climate Change experiment (CalNex; Ryerson et al., 2013) on the NOAA P-3—and present measurement comparisons with other onboard sensors and flask samplers. We describe operations of the QCLS and the calibrations of the carbon and greenhouse-gas measurements of CO₂, CH₄, N₂O, and CO. We evaluate the traceability of calibration standards from the World Meteorological Organization (WMO) and National Oceanic and Atmospheric Administration (NOAA) calibrated values to the in-flight standards as well as long-term sensor stability. NOAA ESRL GMD is the Central Calibration Laboratory (CCL) for the WMO’s Global Atmospheric Watch (GAW) for the atmospheric trace gases CO₂, CH₄, N₂O, and CO. WMO CCL is responsible for maintaining and distributing the WMO Mole Fraction scale for a specified gas in air (<http://www.esrl.noaa.gov/gmd/ccl/>). We then characterize the in-flight drift through interpolations to periodic sample replacements with calibrated air and discuss how this affects our overall accuracy. In the context of traceability and sensor accuracy,

Evaluation of the Airborne Quantum Cascade Laser Spectrometer (QCLS)

G. W. Santoni et al.

Title Page

Abstract

Introduction

Conclusions

References

Tables

Figures

⏪

⏩

◀

▶

Back

Close

Full Screen / Esc

Printer-friendly Version

Interactive Discussion

long-term drift, standard additions can offset inaccuracies due to pressure and temperature fluctuations. The Allan variance, a measure of the precision of a sensor as a function of averaging time (Werle et al., 1993), can be used to quantify both the short-term (e.g., electronic noise) and long-term precision of a sensor as well as the drift.

Figure 2 shows the in-flight Allan variance for the CO₂, CH₄, N₂O, and CO measurements from the QCLS with 1 s RMS precisions (Allan standard deviations) of 20, 0.5, 0.09, and 0.15 ppb, respectively. The measurements shown in Fig. 2 were taken during a section of HIPPO that sampled a relatively constant air mass above the remote Pacific Ocean. This is the same section of data presented in the supplementary material section of Kort et al. (2011). Table 1 summarizes the Allan precisions at 1, 10, and 100 s for the 4 species. During flight sampling, the Allan precision between 1 and 10 s improves for all species, but only continues to improve between 10 and 100 s for N₂O. This is largely because atmospheric variability in CO₂, CH₄, and CO is larger relative to N₂O as the atmospheric lifetime of N₂O is ~ 118 yr (Hsu and Prather, 2010) and the sources are more spatially uniform than for the other species. Because of this, Table 1 also includes the Allan precision from laboratory tests that sampled air continuously flowing from calibration cylinders with near-ambient atmospheric concentrations.

The flow schematics for QCLS-CO₂ are shown in Fig. 3. The two schematics are very similar. QCLS-CO₂ and QCLS-DUAL have independent inlets. On the HIAPER-GV, both inlets extend out from the QCLS rack to a dedicated NCAR HIAPER Modular Inlet (HIMIL) mounted to the edge of the aircraft. The HIMIL extends the inlet 28 cm from the body of the aircraft (NCAR, 2005) and the two QCLS inlets, both 316 stainless steel 0.25" OD, sample from within the center flow path, oriented away from the direction of flow (i.e. rear-facing). This orientation minimizes large particle entrainment and protects the sampling system from liquid water and ice. For the NOAA P-3 aircraft, the inlets both consist of stainless steel 3/8" OD tubing smoothly bent at 90° to be parallel to the aircraft and oriented at 135° relative to the horizontal direction of flight. Once the sample enters the body of both aircraft, the two sample lines consist of ~ 1.5 m of Synflex type 1300 tubing (6.35 mm = 1/4" OD for QCLS-CO₂ and 9.525 cm = 3/8" OD for

Evaluation of the Airborne Quantum Cascade Laser Spectrometer (QCLS)

G. W. Santoni et al.

Title Page

Abstract

Introduction

Conclusions

References

Tables

Figures

⏪

⏩

◀

▶

Back

Close

Full Screen / Esc

Printer-friendly Version

Interactive Discussion

the low-span and high-span “targets” one after the other and use all four primary cylinders. Because use of the primary cylinders with QCLS required the instrument to be in a laboratory setting, we were able to perform gas-deck calibrations only before or after a given deployment. When the small cylinders in the gas decks reached 500 psi, they were flushed (3X) and filled with calibration air from AL secondary cylinders. For HIPPO, the refills would take place in Christchurch, NZ, using a different set of secondary cylinders than the secondary cylinders used to fill the gas decks on the first half (southbound) set of the HIPPO flight circuit. We would therefore calibrate the gas deck after filling it but before using in on the southbound flights, and after both filling it and using it on the second half northbound set of the HIPPO flight circuit. Because of these logistics, the calibration values calculated during gas-deck calibrations were only used as a check against filling error, ensuring that the gas-deck values fell within 3σ of the uncertainty attributed to the secondary tank calibration (Fig. 5) from the NOAA primary cylinders. For consistency, and because calibrations of the gas decks themselves required the use of the primary cylinders, the calibration values assigned to the air in the gas decks were always the values from the secondary cylinder calibrations shown in Fig. 5. Figure 5 also shows that, within uncertainty, there is no evidence of drift in the secondary cylinders from 2010 to 2012.

In-flight data are then tied to the NOAA scale by periodic sample replacement with air from the gas decks. The sampling structure is shown in Fig. 6. Within a given 60 min, the calibration sequences is as follows: minutes 7–9, 22–24, 37–39, 52–54 sampled zero/reference, minutes 9–10 and 39–40 sampled low-span, minutes 10–11 and 40–41 sampled high-span, and minutes 41–42 sampled a check-span. Because of the different equilibration times for the different species, we changed the order of the LS and HS additions to occur before the zero-air additions (see below). The zero was sampled most frequently at 15 min intervals to track QCLS drift. The low and high-spans were sampled at 30 min intervals, and the reference-span was sampled every hour for one minute. For a given hour of flight, the effective sampling duty cycle was therefore $\sim 78\%$ (47 min of sampling per hour). The calibrations for QCLS-DUAL and

by sampling the zero-air for 2 min, sampling the LS and HS before sampling the zero-air, and using a smaller sampling window to calculate the zero-air spectroscopically-calibrated mixing ratios of N₂O, as seen in Fig. 6.

Using a reference calibration cylinder (one with near-ambient atmospheric concentrations, e.g. CC56519 in Table 2b) instead of a zero to track instrument stability would minimize the effect of this problem. Because this tank is used so frequently to track drift, however, it would have been impractical to use, particularly on HIPPO where opportunities to ship calibration tanks and refill the gas decks are limited. We tested this assumption on one flight during HIPPO V (RF14; 9 September 2011) and showed that using a 1 min equilibration time for a reference tank at ambient concentrations gave nearly equivalent results as using a zero-air tank for 2 min.

It should be noted that the boiling point of CO₂ (−57 °C) is even higher than that of N₂O, so this effect is equally important for CO₂ and can be observed in Fig. 6. However, it matters to a much smaller extent as the Synflex is always in contact with air that is very close to ambient.

To distinguish sampling intervals from calibration intervals, we use an empirical relationship that is a function of ambient pressure and tubing length. These differ for HIPPO and CalNex because of the hardware configurations, notably the use of the HIMIL on HIPPO. For HIPPO and QCLS-DUAL, we calculate experimental delay times from the HIMIL to the calibration-addition point just downstream of the inlet filter (Fig. 3) as a linear function of ambient pressure in the HIMIL. We also calculate a time delay corresponding to the equilibration time from that point to the measurement cell as a quadratic function of ambient pressure in the HIMIL. These have the functional form:

$$t_{\text{delay}} = 1.6201 \cdot P_{\text{amb}} \quad (1)$$

$$t_{\text{equil}} = 0.02763 \cdot P_{\text{amb}}^2 + 0.14993 \cdot P_{\text{amb}} + 3.75488 \quad (2)$$

Evaluation of the Airborne Quantum Cascade Laser Spectrometer (QCLS)

G. W. Santoni et al.

Title Page

Abstract

Introduction

Conclusions

References

Tables

Figures

⏪

⏩

◀

▶

Back

Close

Full Screen / Esc

Printer-friendly Version

Interactive Discussion



Evaluation of the Airborne Quantum Cascade Laser Spectrometer (QCLS)

G. W. Santoni et al.

Title Page

Abstract

Introduction

Conclusions

References

Tables

Figures

◀

▶

◀

▶

Back

Close

Full Screen / Esc

Printer-friendly Version

Interactive Discussion



where time and pressure have units of s and psi. The dynamic range of ambient pressure is much smaller in CalNex and does not include a HIMIL, which affects the pressure at the inlet, so the equilibration time for CalNex is treated as a constant value derived from plume comparisons between QCLS and a fast-response black-carbon measurement (Schwarz et al., 2010) that was available for both HIPPO and CalNex. Equations for QCLS-CO₂ have different coefficients but the same form. The equations were calculated empirically during several test flights on each campaign and then held constant throughout each campaign.

The HIMIL port, designed to slow air-flow, complicated the instrument equilibration time but dampened the input pressure variability of the sample. For CalNex, however, the variability in the sample pressure was occasionally not adequately controlled by the pressure control elements. Certain fluctuations in pressure were able to propagate to the QCLS-DUAL sample cell and affect the measurements. The effect of this cell “ringing” was most apparent in the N₂O measurement which occasionally showed high-frequency (1 Hz) positive and negative excursions of > 1 – 2 ppb for N₂O, a trace that should only see negative excursions in stratospheric air. We apply a filter which removed measurements in which the 1 Hz rate change of pressure is greater than 3 standard deviations of the mean ($\sigma = 0.16 \text{ hPa s}^{-1}$). This resulted in an effective duty cycle that was 3 % lower than without the pressure filter, but removed spurious spikes in the data.

Calibration time intervals were determined using these functions and the solenoid valve actuation time, and a mean mixing ratio for each sample addition was calculated in a given window. The zero-air values measured every 15 min were then fit using a penalized Akima spline interpolation technique (Akima, 1970) to evaluate the drift of the instrumentation. Other filters, such as loess and spline smoothers, occasionally cause severe curvature in the interpolation, particularly near the beginning of flight where sensors may not be fully equilibrated. This zero-air Akima-spline is evaluated at all the 1 Hz sampling times and subtracted from the entire dataset. Using the zero-air Akima-spline-subtracted data for the QCLS-DUAL species (for example, CH_{4,Zraw}),

the mean values of each low-span and high-span window are interpolated using the same Akima-spline to the measurement times. $\text{CH}_{4,Z_{\text{raw}}}$ is then linearly interpolated to the low-span Akima-spline and high-span Akima-spline ($\text{CH}_{4,Z_{\text{ALS}}}$ and $\text{CH}_{4,Z_{\text{AHS}}}$, respectively) according to:

$$\text{CH}_{4,\text{cal}} = \left(\frac{\text{CH}_{4,Z_{\text{raw}}} - \text{CH}_{4,Z_{\text{ALS}}}}{\text{CH}_{4,Z_{\text{AHS}}} - \text{CH}_{4,Z_{\text{ALS}}}} \right) \cdot (\text{CH}_{4,\text{HS}_{\text{VAL}}} - \text{CH}_{4,\text{LS}_{\text{VAL}}}) + \text{CH}_{4,\text{LS}_{\text{VAL}}} \quad (3)$$

where $\text{CH}_{4,\text{LS}_{\text{VAL}}}$ and $\text{CH}_{4,\text{HS}_{\text{VAL}}}$ are the two constant values of the low-span and high-span secondary AL calibration cylinders used to fill the gas-deck (Table 2b). The equations for N_2O and CO are equivalent and generate the calibrated sample dry-air mole fractions ($\text{CH}_{4,\text{cal}}$ in Eq. 3). Figure 8 shows the different Akima-splines for an arbitrary flight during HIPPO 5, along with the ambient pressure for the 4 species. The axes are all scaled such that the different tracers – zero-air, low-span, high-span, and reference air – from the gas decks have equivalent ordinate ranges. The CO_2 trace in Fig. 8 is in units of ppb relative to the reference, meaning that a value of $-17\,500$, corresponds to the low-span that is 17.5 ppm lower than the near-ambient reference. Figure 8 is a standard output product of the batch processing and is purposely scaled to emphasize the fluctuations of calibration standards over the course of a given flight. Because of the linear interpolation between the zero-subtracted low-span and high-span, the relative fluctuation of those two standards has the largest effect on the effective calibrated measurements.

The CO_2 calibration additions shown in Fig. 8 are treated in a slightly different fashion than the QCLS-DUAL species. Because QCLS- CO_2 is a differential measurement and the range of observations is the largest of any species (in terms of concentration changes measured over the course of a flight), the CO_2 interpolation is not calculated linearly. Instead, we take the median of the low-span, reference, and high-span values calculated over the course of any particular flight and fit a quadratic function to those median values for that flight. The reference-subtracted measurements are then quadratically interpolated using this fixed function. We experimented with different

Evaluation of the Airborne Quantum Cascade Laser Spectrometer (QCLS)

G. W. Santoni et al.

Title Page

Abstract

Introduction

Conclusions

References

Tables

Figures



Back

Close

Full Screen / Esc

Printer-friendly Version

Interactive Discussion



Evaluation of the Airborne Quantum Cascade Laser Spectrometer (QCLS)

G. W. Santoni et al.

Title Page

Abstract

Introduction

Conclusions

References

Tables

Figures

◀

▶

◀

▶

Back

Close

Full Screen / Esc

Printer-friendly Version

Interactive Discussion

analyzer, which measures molecular absorption of CO₂ in a sample stream relative to a reference stream of air. Because it is a nondispersive analyzer, the measurement is sensitive to different parts of the molecular absorption band of CO₂. Tohjima et al. (2009) characterized the sensitivity of 3 Licors (two 6252 and one 6262) to each of the isotopologues of CO₂. They use a Relative Molar Response (RMR) value for each isotopologue to calculate the effective change in concentration determined for each isotopologue (see their Table 4). Given a hypothetical CO₂ mixing ratio of 400 ppm, the isotopic abundances in HITRAN (Rothman et al., 2007) can be used to approximate the individual mixing ratios of the three dominant isotopologue – ¹⁶O¹²C¹⁶O, ¹⁶O¹³C¹⁶O, and ¹⁶O¹²C¹⁸O – as 393.68160, 4.42296 and 1.57883 ppm, respectively. The sum of these three concentrations is less than 400 (399.68339) as other minor isotopes contribute to the total concentration. Atmospheric CO₂ has an approximate isotopic composition of δ¹³C = −10‰ and δ¹⁸O = 40‰, where these quantities are calculated according to:

$$\delta^{13}\text{C}_{\text{CO}_2} = \left[\frac{\text{R13}_{\text{sam}}}{\text{R13}_{\text{vpdb}}} - 1 \right] \cdot 1000 \quad (4)$$

$$\delta^{18}\text{C}_{\text{CO}_2} = \left[\frac{\text{R18}_{\text{sam}}}{\text{R18}_{\text{vsmow}}} - 1 \right] \cdot 1000 \quad (5)$$

where R13 represents the ratio of ¹³C to ¹²C in a sample of CO₂ or in the standard Vienna Pee Dee Belemnite (vpdb = 0.011180) and R18 represents the ratio of ¹⁸O to ¹⁶O in CO₂ or in Standard Mean Ocean Water (smow = 0.0020052). Using these equations, we can calculate atmospheric values for R13 and R18 of 0.0110682 and 0.002085408, respectively. The abundance of the dominant isotopologue (¹²C¹⁶O¹⁶O), excluding minor isotopes, must therefore be 1 minus the R13 and twice the R18 abundances, or 0.984761, which corresponds to a concentration of 393.592606. Because QCLS-CO₂ only scans across one absorption line for the dominant isotopologue (mass 44), calibration additions using cylinders with non-atmospheric isotopic composition can therefore

Evaluation of the Airborne Quantum Cascade Laser Spectrometer (QCLS)

G. W. Santoni et al.

Title Page

Abstract

Introduction

Conclusions

References

Tables

Figures

⏪

⏩

◀

▶

Back

Close

Full Screen / Esc

Printer-friendly Version

Interactive Discussion

result in biases in the measurements. A hypothetical tank that has a total CO₂ concentration of 400 ppm and isotopic composition of $\delta^{13}\text{C} = -35\text{‰}$ and $\delta^{18}\text{O} = 10\text{‰}$ (typical of a Scott–Marrin cylinder) will have dominant isotopologue $^{16}\text{O}^{12}\text{C}^{16}\text{O}$, $^{16}\text{O}^{13}\text{C}^{16}\text{O}$, and $^{16}\text{O}^{12}\text{C}^{18}\text{O}$ concentrations of 393.752405, 4.312064 and 1.618919 ppm, the sum of which is still 399.68339. But the concentration of the $^{12}\text{C}^{16}\text{O}_2$ isotopologue is higher by 0.1598 ppm compared to the concentration with near-atmospheric isotopic composition. This must be accounted for in relating calibration cylinder values to sample concentrations.

The mean RMR corrections for the three dominant isotopologues from the two Licor-6252 are (1) the mean of 1.0073 and 1.0040, (2) the mean of 0.21 and 0.45, and (3) the mean of 1.26 and 1.43, which are multiplied by the difference in isotopologue concentrations between the 400 ppm cylinder and the 400 ppm atmospheric sample. When summed, the mean value is -0.059 ppm with a range over the two instruments of -0.041 to -0.077 ppm. Chen et al. (2010) calculated a similar value using specific isotopic composition of the tanks of -0.09 ppm.

To account for the combined effect on the QCLS-CO₂ calibration, the -0.059 ppm and the 0.1598 values must be added to the retrieved sample mixing ratio. The -0.059 ppm puts the calibration cylinder values calculated using the GSE onto the same isotopic scale as the NOAA primaries (i.e. atmospheric isotopic composition). The 0.1598 value accounts for the fact that QCLS-CO₂ derives a total mixing ratio using the absorption spectrum of the dominant $^{12}\text{C}^{16}\text{O}_2$ isotopologue and the HITRAN abundance, which differs from the atmospheric abundance as shown above. These effects partially offset, but result in a ~ 0.1 ppm bias term, which is important considering that atmospheric concentration gradients are often not much larger than this. The particular isotopic values of the calibration cylinders (Table 2b) were measured by the Stable Isotope Ratio Facility for Environmental Research (SIRFER, University of Utah) and were used to calculate the exact corrections for the tanks. The NOAA primary tanks had near-atmospheric ^{13}C isotopic composition of around -10 to -15‰ , Scott

Specialty tanks usually fell in the -45 to -50% range, and Scott–Marrin usually fell in the -30 to -40% range.

The error for CH_4 due to differing isotopic composition between the atmosphere ($^{13}\text{C} \approx -47\%$) and calibration cylinders ($^{13}\text{C} \approx -30\%$) was calculated to be a ~ 0.3 ppb effect, smaller than the 1 Hz precision. The effects for N_2O and CO were proportionally smaller and these effects are therefore ignored for QCLS-DUAL.

3 Missions and other instrumentation

The QCLS was operated in the same configuration in both CalNex and HIPPO with only minor changes due to the aircraft-specific issues already discussed. We now present comparisons with other coincident instruments, synchronized in time using the STRATUM-1 aircraft data system.

For HIPPO, two additional fast-response (> 1 Hz) CO_2 sensors were available for comparison: the OMS sensor (Daube et al., 2002), and the NCAR Airborne Oxygen Instrument (AO2), which includes a single-cell Licor-820 sensor. Figure 10 shows the 1 Hz measurement difference distribution for QCLS against OMS and AO2 for all HIPPO flights. QCLS- CO_2 and OMS agree to better than 0.05 ppm, with a standard deviation of the difference of 0.37, owing in part to the slower cell response time of OMS. Assuming the sensors have no covariance, the 1 Hz OMS precision of 0.1 ppm and the 1 Hz QCLS precision of 0.02 ppm would sum in quadrature for an expected precision of 0.1 ppm. The actual distribution is 0.37 ppm, roughly a factor of 4 higher. The AO2 instrument has a 1-sigma, 1 s precision of ~ 0.6 ppm. QCLS- CO_2 and AO2 agree to within 0.15 ppm and have an even larger variance on the distribution of the measurement differences. It is important to note that many unresolved biases spanning one hour or an entire flight exist among the CO_2 sensors on HIPPO and tend to average out as presented in Fig. 10. The Research Aviation Facility (RAF) vacuum ultraviolet (VUV) CO sensor is the only other fast-response instrument measuring one

Evaluation of the Airborne Quantum Cascade Laser Spectrometer (QCLS)

G. W. Santoni et al.

Title Page

Abstract

Introduction

Conclusions

References

Tables

Figures

◀

▶

◀

▶

Back

Close

Full Screen / Esc

Printer-friendly Version

Interactive Discussion

of the QCLS species (Gerbig et al., 1999). That comparison, also shown in Fig. 10, shows a bias of 1.8 ppb over the HIPPO mission.

Two onboard gas chromatographs – the Unmanned Aircraft Systems (UAS) Chromatograph for Atmospheric Trace Species (UCATS, Moore et al., 2003; Fahey et al., 2006; Wofsy et al., 2011) and the PAN and other Trace Hydrohalocarbon Experiment (PANTHER; Elkins et al., 2002; Wofsy et al., 2011) – measured a variety of chemical species including CH₄, N₂O, and CO. Figure 11 shows the one-to-one comparison of the QCLS to PANTHER (top) and UCATS (bottom) after applying the averaging kernel of each GC to the 1 Hz QCLS data. In addition to the in situ data, sparser flask measurements from the NOAA Whole Air Sampler (NWAS) are compared in Fig. 12. The axis ranges on Figs. 11 and 12 are the same, with the exception of N₂O, which has large variability from the GC-based measurements. Table 4 summarizes the median differences with NOAA for each of the QCLS species at the mean concentration measured on each of the 5 HIPPO transects. Mean biases calculated over the course of HIPPO are -112, 0.85, 1.07, and -1.94 ppb for the 4 species. Only N₂O falls outside of the estimated uncertainties in the measurements. This is in part due to the recalibration of primary cylinder 4 (Table 2a) that deviated from the original value by more than 4 times the 1 σ NOAA calibration uncertainty. This cylinder falls on the high range of the NOAA N₂O calibration standards and is only bracketed by one NOAA standard with higher concentration (Hall et al., 2007). Additional CO₂ flask data was available from the NCAR/Scripps Medusa flask sampler which collected air in 1.5 L glass flasks for analysis in the Scripps Oxygen Laboratory. Table 5 presents the corresponding median differences between QCLS and Medusa at the mean concentration measured on each of the 5 HIPPO transects. Although the CO₂ offsets for individual missions to Scripps are not correlated with the offsets to NOAA, the 5-mission average is very similar at -108 ppb.

For CalNex, the payload of the NOAA P-3 aircraft included simultaneous 1 Hz measurements of CO using the NOAA VUV spectrometer (Holloway et al., 2000) and CO₂ and CH₄ using the NOAA/Picarro Cavity Ring-Down Spectrometer (CRDS). The

Evaluation of the Airborne Quantum Cascade Laser Spectrometer (QCLS)

G. W. Santoni et al.

Title Page

Abstract

Introduction

Conclusions

References

Tables

Figures



Back

Close

Full Screen / Esc

Printer-friendly Version

Interactive Discussion

Evaluation of the Airborne Quantum Cascade Laser Spectrometer (QCLS)

G. W. Santoni et al.

Title Page

Abstract

Introduction

Conclusions

References

Tables

Figures

⏪

⏩

◀

▶

Back

Close

Full Screen / Esc

Printer-friendly Version

Interactive Discussion

comparisons for all three species are shown in Fig. 13. No additional sensors measured N_2O during CalNex. The CRDS made 1-Hz measurements of CO_2 and CH_4 with 1 s RMS precisions of 100 and 1.5 ppb, respectively (Peischl et al., 2012). Both sets of measurements were independently calibrated to NOAA standards during flight, accounting for roughly 20 % of the sampling duty cycle for each instrument. The QCLS and CRDS CO_2 data agreed well with one another, with a mean difference of 0.05 ppm and standard deviation of 0.51 over 130 flight hours of sampling, similar to the QCLS and OMS comparison on HIPPO. The mean difference in CH_4 was 4.5 ppb, more than our estimated uncertainty, with a standard deviation of 5.1 ppb. The cause of the CH_4 measurement discrepancy has remained a mystery despite extensive efforts to explain the difference. These biases correspond to errors of 0.01 % and 0.25 % for CO_2 and CH_4 , respectively, using background concentrations of 390 ppm and 1800 ppb. The bias between the independent CO sensors was 1.1 ppb during CalNex. It should be noted that the NOAA VUV CO sensor did not dry the ambient air during measurement and reported wet mole fractions. Dilution therefore accounts for some of the bias. The in-flight NOAA VUV CO measurements were calibrated by means of standard additions traceable to NIST with backgrounds determined by catalytically scrubbing CO from the ambient air sample.

To minimize data gaps in the 1 Hz flight data over the missions, we fit a loess curve with a 1000 s span window to calculate the time-evolution of the QCLS minus OMS/CRDS/VUV concentration bias. The QCLS data is used as the primary data, and calibration gaps are filled using the sum of the OMS/CRDS/VUV data and the loess bias curve for ($\text{CO}_2.X$ in HIPPO, $\text{CO}_2.X$ and $\text{CH}_4.X$ in CalNex, and $\text{CO}.X$ in both HIPPO and CalNex). This resulted in an overall mission data retrieval duty cycle of over 95 % for HIPPO and 97 % for CalNex, a significant improvement over the ~ 78 % duty cycle from QCLS alone. These merge products are denoted $\text{CO}_2.X$, $\text{CH}_4.X$, and $\text{CO}.X$. A merge product for N_2O was not created because no other fast-response N_2O sensors were available for either mission.

4 Conclusions

We have achieved airborne measurement compatibilities with respect to WMO/NOAA scales of 0.03 %, 0.05 %, 0.3 %, and 2 % for CO₂, CH₄, N₂O, and CO relative to background concentrations of 390 ppm, 1850 ppb, 325 ppb, and 100 ppb, respectively, by adequately regulating pressure and temperature and by using a robust in-flight calibration procedure that improves upon spectroscopically-calibrated measurements. We report long-term compatibility for CO₂, CH₄, N₂O, and CO from nearly 450 flight hours of 100, 1, 1.1, and 2 ppb, respectively. The datasets generated using the QCLS for HIPPO and CalNex have provided extensive global (HIPPO) and regional (CalNex) coverage and have been useful in many studies to date (Graven et al., 2013; Wunch et al., 2010; Kort et al., 2011, 2012; Wecht et al., 2012; Xiang et al., 2013b; Peischl et al., 2012). We emphasize the importance of in-flight calibrations traceable to WMO/NOAA standards, essential in studies that combine measurements from independent sensors, and present our practices for their implementation.

Acknowledgements. We would like to add a first sentence to the acknowledgments: “The Harvard QCLS was a joint collaboration with Aerodyne and NCAR, and was funded by NSF as a core instrument on NCAR’s Gulfstream V aircraft.”

References

- Chen, H., Winderlich, J., Gerbig, C., Hoefler, A., Rella, C. W., Crosson, E. R., Van Pelt, A. D., Steinbach, J., Kolle, O., Beck, V., Daube, B. C., Gottlieb, E. W., Chow, V. Y., Santoni, G. W., and Wofsy, S. C.: High-accuracy continuous airborne measurements of greenhouse gases (CO₂ and CH₄) using the cavity ring-down spectroscopy (CRDS) technique, *Atmos. Meas. Tech.*, 3, 375–386, doi:10.5194/amt-3-375-2010, 2010.
- Daube, B. C., Boering, K. A., Andrews, A. E., and Wofsy, S. C.: A high-precision fast-response airborne CO₂ analyzer for in situ sampling from the surface to the middle stratosphere, *J. Atmos. Oceanic Technol.*, 19, 1532–1543, 2002.

AMTD

6, 9689–9734, 2013

Evaluation of the Airborne Quantum Cascade Laser Spectrometer (QCLS)

G. W. Santoni et al.

Title Page

Abstract

Introduction

Conclusions

References

Tables

Figures

◀

▶

◀

▶

Back

Close

Full Screen / Esc

Printer-friendly Version

Interactive Discussion

Evaluation of the Airborne Quantum Cascade Laser Spectrometer (QCLS)

G. W. Santoni et al.

Title Page

Abstract

Introduction

Conclusions

References

Tables

Figures

◀

▶

◀

▶

Back

Close

Full Screen / Esc

Printer-friendly Version

Interactive Discussion

- Dlugokencky, E. J., Myers, R. C., Lang, P. M., Masarie, K. A., Crotwell, A. M., Thoning, K. W., Hall, B. D., Elkins, J. W., and Steele, L. P.: Conversion of NOAA atmospheric dry air CH₄ mole fractions to a gravimetrically prepared standard scale, *J. Geophys. Res.-Atmos.*, 110, D18306, doi:10.1029/2005JD006035, 2005.
- 5 Elkins, J. W., Moore, F. L., and Kline, E. S.: Update: new airborne gas chromatograph for NASA airborne platforms, in: *Proceedings of the Earth Science Technology Conference*, 11–13 June 2002, Pasadena, 1–3, 2002.
- Fahey, D. W., Churnside, J. H., Elkins, J. W., Gasiewski, A. J., Rosenlof, K. H., Summers, S., Aslaksen, M., Jacobs, T. A., Sellars, J. D., Jennison, C. D., Freuding, L. C., and Cooper, M.:
 10 Altair unmanned aircraft system achieves demonstration goals, *EOS Transactions American Geophysical Union*, 87, 197–201, doi:10.1029/2006EO200002, 2006.
- Fried, A., Diskin, G., Weibring, P., Richter, D., Walega, J. G., Sachse, G., Slate, T., Rana, M., and Podolske, J.: Tunable infrared laser instruments for airborne atmospheric studies, *Appl. Phys. B-Lasers O.*, 92, 409–417, 2009.
- 15 Gerbig, C., Schmitgen, S., Kley, D., Volz-Thomas, A., Dewey, K., and Haaks, D.: An improved fast-response vacuum-UV resonance fluorescence CO instrument, *J. Geophys. Res.-Atmos.*, 104, 1699–1704, doi:10.1029/1998JD100031, 1999.
- Gerbig, C., Lin, J. C., Wofsy, S. C., Daube, B. C., Andrews, A. E., Stephens, B. B., Bakwin, P. S., and Grainger, C. A.: Toward constraining regional-scale fluxes of CO₂ with atmospheric ob-
 20 servations over a continent: 2. Analysis of COBRA data using a receptor-oriented framework, *J. Geophys. Res.*, 108, 4757, doi:10.1029/2003JD003770, 2003.
- Graven, H. D., Keeling, R. F., Piper, S. C., Patra, P. K., Stephens, B. B., Wofsy, S. C., Welp, L. R., Sweeney, C., Tans, P. P., Kelley, J. J., Daube, B. C., Kort, E. A., Santoni, G. W., and Bent, J. D.: Enhanced seasonal exchange of CO₂ by northern ecosystems since 1960, *Science*, 341,
 25 1085–1089, doi:10.1126/science.1239207, 2013.
- Hall, B. D., Dutton, G. S., and Elkins, J. W.: The NOAA nitrous oxide standard scale for atmospheric observations, *J. Geophys. Res.-Atmos.*, 112, D09305, doi:10.1029/2006JD007954, 2007.
- Holloway, J. S., Jakoubek, R. O., Parrish, D. D., Gerbig, C., Volz-Thomas, A., Schmitgen, S.,
 30 Fried, A., Wert, B., Henry, B., and Drummond, J. R.: Airborne intercomparison of vacuum ultraviolet fluorescence and tunable diode laser absorption measurements of tropospheric carbon monoxide, *J. Geophys. Res.-Atmos.*, 105, 24251–24261, doi:10.1029/2000JD900237, 2000.

**Evaluation of the
Airborne Quantum
Cascade Laser
Spectrometer (QCLS)**

G. W. Santoni et al.

Title Page

Abstract

Introduction

Conclusions

References

Tables

Figures

◀

▶

◀

▶

Back

Close

Full Screen / Esc

Printer-friendly Version

Interactive Discussion



Hsu, J. and Prather, M. J.: Global long-lived chemical modes excited in a 3-D chemistry transport model: stratospheric N_2O , NO_y , O_3 , and CH_4 chemistry, *Geophys. Res. Lett.*, 37, L07805, doi:10.1029/2009GL042243, 2010.

Jiménez, R., Herndon, S., Shorter, J. H., Nelson, D. D., McManus, J. B., and Zahniser, M. S.: Atmospheric trace gas measurements using a dual quantum-cascade laser mid-infrared absorption spectrometer, *Proc. SPIE*, 318, 5738, doi:10.1117/12.597130, 2005.

Jiménez, R., Park, S., Daube, B. C., McManus, J. B., Nelson, D. D., Zahniser, M. S., and Wofsy, S. C.: A new quantum-cascade laser based spectrometer for high-precision airborne CO_2 measurements, *WMO/GAW Reports*, 168, 100–105, 2006.

Kort, E. A., Patra, P. K., Ishijima, K., Daube, B. C., Jimenez, R., Elkins, J., Hurst, D., Moore, F. L., Sweeney, C., and Wofsy, S. C.: Tropospheric distribution and variability of N_2O : evidence for strong tropical emissions, *Geophys. Res. Lett.*, 38, L15806, doi:10.1029/2011GL047612, 2011.

Kort, E. A., Wofsy, S. C., Daube, B. C., Diao, M., Elkins, J. W., Gao, R. S., Hints, E. J., Hurst, D. F., Jiménez, R., Moore, F. L., Spackman, J. R., and Zondlo, M. A.: Atmospheric observations of Arctic Ocean methane emissions up to 82°N , *Nature Geosci.*, 5, 318–321, doi:10.1038/ngeo1452, 2012.

McManus, J. B., Kebedian, P. L., and Zahniser, W. S.: Astigmatic mirror multi-pass absorption cells for long-path-length-spectroscopy, *Appl. Optics*, 34, 3336–3348, doi:10.1364/AO.34.003336, 1995.

Miller, S. M., Matross, D. M., Andrews, A. E., Millet, D. B., Longo, M., Gottlieb, E. W., Hirsch, A. I., Gerbig, C., Lin, J. C., Daube, B. C., Hudman, R. C., Dias, P. L. S., Chow, V. Y., and Wofsy, S. C.: Sources of carbon monoxide and formaldehyde in North America determined from high-resolution atmospheric data, *Atmos. Chem. Phys.*, 8, 7673–7696, doi:10.5194/acp-8-7673-2008, 2008.

Moore, F. L., Elkins, J. W., Ray, E. A., Dutton, G. S., Dunn, R. E., Fahey, D. W., McLaughlin, R. J., Thompson, T. L., Romashkin, P. A., Hurst, D. F., and Wamsley, P. R.: Balloonborne in situ gas chromatograph for measurements in the troposphere and stratosphere, *J. Geophys. Res.*, 108, 8330, doi:10.1029/2001JD000891, 2003.

NCAR, UCAR, RAF: NCAR HIAPER Modular Inlet – HIMIL available at: <http://www.eol.ucar.edu/~dcrogers/HIAPER/Inlets/HIMIL/> (last access: 10 November 2013), 2005.

Nelson, D. D., McManus, J. B., Urbanski, S., Herndon, S., and Zahniser, M. S.: High precision measurements of atmospheric nitrous oxide and methane using thermoelectrically cooled

Evaluation of the Airborne Quantum Cascade Laser Spectrometer (QCLS)

G. W. Santoni et al.

Title Page

Abstract

Introduction

Conclusions

References

Tables

Figures

◀

▶

◀

▶

Back

Close

Full Screen / Esc

Printer-friendly Version

Interactive Discussion

mid-infrared quantum cascade lasers and detectors, *Spectrochim. Acta A*, 60, 3325–3335, 2004.

Novelli, P. C., Collins, J. E. J., Myers, R. C., Sachse, G. W., and Scheel, H. E.: Reevaluation of the NOAA/CMDL carbon monoxide reference scale and comparisons with CO reference gases at NASA-Langley and the Fraunhofer Institute, *J. Geophys. Res.-Atmos.*, 99, 12833–12839, 1994.

O'Shea, S. J., Bauguitte, S. J.-B., Gallagher, M. W., Lowry, D., and Percival, C. J.: Development of a cavity-enhanced absorption spectrometer for airborne measurements of CH₄ and CO₂, *Atmos. Meas. Tech.*, 6, 1095–1109, doi:10.5194/amt-6-1095-2013, 2013.

Peischl, J., Ryerson, T. B., Holloway, J. S., Trainer, M., Andrews, A. E., Atlas, E. L., Blake, D. R., Daube, B. C., Dlugokencky, E. J., Fischer, M. L., Goldstein, A. H., Guha, A., Karl, T., Kofler, J., Kosciuch, E., Misztal, P. K., Perring, A. E., Pollack, I. B., Santoni, G. W., Schwarz, J. P., Spackman, J. R., Wofsy, S. C., and Parrish, D. D.: Airborne observations of methane emissions from rice cultivation in the Sacramento Valley of California, *J. Geophys. Res.*, 117, D00V25, doi:10.1029/2012JD017994, 2012.

Rothman, L. S., Gordon, I. E., Barbe, A., Benner, D. Chris, Bernath, P. F., Birk, M., Boudon, V., Brown, L. R., Campargue, A., Champion, J.-P., Chance, K., Coudert, L. H., Dana, V., Devi, V. M., Fally, S., Flaud, J.-M., Gamache, R. R., Goldman, A., Jacquemart, D., Kleiner, I., Lacome, N., Lafferty, W. J., Mandin, J.-Y., Massie, S. T., Mikhailenko, S. N., Miller, C. E., Moazzen-Ahmadi, N., Naumenko, O. V., Nikitin, A. V., Orphal, J., Perevalov, V. I., Perrin, A., Predoi-Cross, A., Rinsland, C. P., Rotger, M., Šimecková, M., Smith, M. A. H., Sung, K., Tashkun, S. A., Tennyson, J., Toth, R. A., Vandaele, A. C., and Vander Auwera, J.: The HITRAN 2008 molecular spectroscopic database, *J. Quant. Spectrosc. Ra.*, 110, 533–572, 2009.

Ryerson, T. B., Andrews, A. E., Angevine, W. M., Bates, T. S., Brock, C. A., Cairns, B., Cohen, R. C., Cooper, O. R., de Gouw, J. A., Fehsenfeld, F. C., Ferrare, R. A., Fischer, M. L., Flagan, R. C., Goldstein, A. H., Hair, J. W., Hardesty, R. M., Hostetler, C. A., Jimenez, J. L., Langford, A. O., McCauley, E., McKeen, S. A., Molina, L. T., Nenes, A., Oltmans, S. J., Parrish, D. D., Pederson, R. B., Pierce, K., Prather, P. K., Quinn, J. H., Seinfeld, C. J., Senff, A., Sorooshian, J. R., Stutz, J., Surratt, J. D., Trainer, M., Volkamer, R., Williams, E. J., and Wofsy, S. C.: The 2010 California Research at the Nexus of Air Quality and Climate Change (CalNex) field study, *J. Geophys. Res.-Atmos.*, 118, 1–37, doi:10.1002/jgrd.50331, 2013.

**Evaluation of the
Airborne Quantum
Cascade Laser
Spectrometer (QCLS)**

G. W. Santoni et al.

Title Page

Abstract

Introduction

Conclusions

References

Tables

Figures

◀

▶

◀

▶

Back

Close

Full Screen / Esc

Printer-friendly Version

Interactive Discussion

Santoni, G. W., Xiang, B., Kort, E. A., Daube, B. C., Andrews, A. E., Sweeney, C., Wecht, K. J., Peischl, J., Ryerson, T. B., Angevine, W. M., Trainer, M., Nehr Korn, T., Eluszkiewicz, J., Jeong, S., Fischer, M. L., Ferrare, R. A., and Wofsy, S. C.: California's methane budget derived from CalNex P-3 aircraft observations and a lagrangian transport model, *J. Geophys. Res.*, in review, 2013.

Schwarz, J. P., Spackman, J. R., Gao, R. S., Watts, L. A., Stier, P., Schulz, M., Davis, S. M., Wofsy, S. C., and Fahey, D. W.: Global-scale black carbon profiles observed in the remote atmosphere and compared to models, *Geophys. Res. Lett.*, 37, L18812, doi:10.1029/2010GL044372, 2010.

Wecht, K. J., Jacob, D. J., Wofsy, S. C., Kort, E. A., Worden, J. R., Kulawik, S. S., Henze, D. K., Kopacz, M., and Payne, V. H.: Validation of TES methane with HIPPO aircraft observations: implications for inverse modeling of methane sources, *Atmos. Chem. Phys.*, 12, 1823–1832, doi:10.5194/acp-12-1823-2012, 2012.

Werle, P., Mücke, R., and Stelm, F.: The limits of signal averaging in atmospheric trace-gas monitoring by tunable diode-laser absorption spectroscopy (TDLAS), *Appl. Phys. B*, 57, 131–139, doi:10.1007/BF00425997, 1993.

Wofsy, S. C. and HIPPO Science Team and Cooperating Modellers and Satellite Teams: HIPPER Pole-to-Pole Observations (HIPPO): fine grained, global scale measurements for determining rates for transport, surface emissions, and removal of climatically important atmospheric gases and aerosols, *Philos. T. R. Soc. A*, 369, 2073–2086, 2011.

Wunch, D., Toon, G. C., Wennberg, P. O., Wofsy, S. C., Stephens, B. B., Fischer, M. L., Uchino, O., Abshire, J. B., Bernath, P., Biraud, S. C., Blavier, J.-F. L., Boone, C., Bowman, K. P., Browell, E. V., Campos, T., Connor, B. J., Daube, B. C., Deutscher, N. M., Diao, M., Elkins, J. W., Gerbig, C., Gottlieb, E., Griffith, D. W. T., Hurst, D. F., Jiménez, R., Keppel-Aleks, G., Kort, E. A., Macatangay, R., Machida, T., Matsueda, H., Moore, F., Morino, I., Park, S., Robinson, J., Roehl, C. M., Sawa, Y., Sherlock, V., Sweeney, C., Tanaka, T., and Zondlo, M. A.: Calibration of the Total Carbon Column Observing Network using aircraft profile data, *Atmos. Meas. Tech.*, 3, 1351–1362, doi:10.5194/amt-3-1351-2010, 2010.

Xiang, B., Miller, S. M., Kort, E. A., Santoni, G. W., Daube, B. C., Commane, R., Angevine, W. M., Ryerson, T. B., Trainer, M. K., Andrews, A. E., Nehr Korn, T., Tian, H., and Wofsy, S. C.: Nitrous oxide (N₂O) emissions from California based on 2010 CalNex airborne measurements, *J. Geophys. Res.-Atmos.*, 118, doi:10.1029/2012JD018244, 2013a.

Evaluation of the Airborne Quantum Cascade Laser Spectrometer (QCLS)

G. W. Santoni et al.

Title Page

Abstract

Introduction

Conclusions

References

Tables

Figures

⏪

⏩

◀

▶

Back

Close

Full Screen / Esc

Printer-friendly Version

Interactive Discussion

- Xiang, B., Nelson, D. D., McManus, J. B., Zahniser, M. S., and Wofsy, S. C.: Towards a stable and absolute atmospheric carbon dioxide instrument using spectroscopic null method, *Atmos. Meas. Tech.*, 6, 1611–1621, doi:10.5194/amt-6-1611-2013, 2013b.
- York, D., Evensen, N. M., Martinez, M. L., and Delgado, J. D. B.: Unified equations for the slope, intercept, and standard errors of the best straight line, *Am. J. Phys.*, 72, 367–375, doi:10.1119/1.1632486, 2004.
- Zahniser, M. S., Nelson, D. D., McManus, J. B., and Keabian, P. L.: Measurement of Trace Gas Fluxes Using Tunable Diode-Laser Spectroscopy, *Philos. T. R. Soc A*, 351, 371–381, 1995.
- Zahniser, M. S., Nelson, D. D., McManus, J. B., Herndon, S. C., Wood, E. C., Shorter, J. H., Lee, B. H., Santoni, G. W., Jimenez, R., Daube, B. C., Park, S., Kort, E. A., and Wofsy, S. C.: Infrared QC laser applications to field measurements of atmospheric trace gas sources and sinks in environmental research: enhanced capabilities using continuous wave QCLs, in: *Proceedings of SPIE – The International Society for Optical Engineering*, 72220H, doi:10.1117/12.815172, 2009.
- Zare, R. N., Kuramoto, D. S., Haase, C., Tan, S. M., Crosson, E. R., and Saad, N. M. R.: High-precision optical measurements of $^{13}\text{C}/^{12}\text{C}$ isotope ratios in organic compounds at natural abundance, *P. Natl. Acad. Sci. USA*, 106 10928–10932, 2009.
- Zhao, C. L. and Tans, P. P.: Estimating uncertainty of the WMO mole fraction scale for carbon dioxide in air, *J. Geophys. Res.-Atmos*, 111, D08s09, doi:10.1029/2005JD006003, 2006.
- Zhao, C., Andrews, A. E., Bianco, L., Eluszkiewicz, J., Hirsch, A., MacDonald, C., Nehrkorn, T., and Fischer, M. L., Atmospheric inverse estimates of methane emissions from Central California, *J. Geophys. Res.*, 114, D16302, doi:10.1029/2008JD011671, 2009.

Evaluation of the Airborne Quantum Cascade Laser Spectrometer (QCLS)

G. W. Santoni et al.

Table 2a. Summary of the primary calibration cylinders used during the CalNex and HIPPO campaigns for QCLS-DUAL. The primary cylinders were filled and calibrated at NOAA in 2005, then recalibrated again after CalNex and before HIPPO IV in 2011. The difference between the two calibrations is shown for each tank and each species.

Name	Cylinder ID	Cal Date	CH ₄ (ppb)		N ₂ O (ppb)		CO (ppb)	
			M.R.	1 σ	M.R.	1 σ	M.R.	1 σ
Primary 1	ND24119	7 Jun 2005	991.8	0.3	154.6	0.2	45.1	0.6
Primary 1	ND24119	30 Jun 2011	995.2	0.3	155.0	0.2	50.4	0.2
			$\Delta = -3.4$		$\Delta = -0.4$		$\Delta = -5.3$	
Primary 2	ND24116	7 Jun 2005	1361.2	0.2	326.92	0.13	102.2	0.4
Primary 2	ND24116	16 Aug 2011	1363.3	0.5	326.92	0.10	103.5	0.7
			$\Delta = -2.1$		$\Delta = 0$		$\Delta = -1.3$	
Primary 3	ND24117	7 Nov 2005	1801.1	0.3	339.2	0.15	352.6	2
Primary 3	ND24117	20 Jun 2011	1801.1	0.2	339.43	0.15	352.9	0.5
			$\Delta = 0$		$\Delta = -0.23$		$\Delta = -0.3$	
Primary 4	ND24118	5 May 2005	2470.9	0.3	356.39	0.15	980.1	10
Primary 4	ND24118	16 Aug 2011	2466.5	1	357.03	0.16	982.4	6.7
			$\Delta = 4.4$		$\Delta = -0.64$		$\Delta = -2.3$	
Primary 5	ND29403	30 Aug 2007	490.5	2.4	248.12	0.10	21.5	0.1
Primary 5	ND29403	21 Jun 2011	486.8	0.2	247.85	0.11	22.7	0.4
			$\Delta = 3.7$		$\Delta = 0.27$		$\Delta = -1.2$	

Title Page

Abstract

Introduction

Conclusions

References

Tables

Figures

◀

▶

◀

▶

Back

Close

Full Screen / Esc

Printer-friendly Version

Interactive Discussion

Evaluation of the Airborne Quantum Cascade Laser Spectrometer (QCLS)

G. W. Santoni et al.

Title Page

Abstract

Introduction

Conclusions

References

Tables

Figures

◀

▶

◀

▶

Back

Close

Full Screen / Esc

Printer-friendly Version

Interactive Discussion

Table 2b. Summary of the secondary calibration cylinders used to fill the gas deck for QCLS-DUAL. Tanks that were used for multiple deployments were recalibrated prior to each use.

Name	Cylinder ID	Date	CH ₄ (ppb)	N ₂ O (ppb)	CO (ppb)
H1/H2 LS	CC12362	20 Nov 2008	1504.94	255.11	34.76
H1/H2 HS	CC81179	20 Nov 2008	1929.76	338.52	201.69
H1/H2/CN LS	CC37815	29 Jan 2010	1672.87	301.55	58.32
H1/H2/CN LS	CC37815	14 Jan 2011	1672.87	301.29	58.57
H1/H2/H3 HS	CC62384	29 Jan 2010	2210.91	354.11	328.84
H1/H2/H3 HS	CC62384	12 Jan 2011	2210.50	353.96	328.91
H3/H4/H5 LS	CC89589	29 Jan 2010	1666.70	298.43	43.75
H3/H4/H5 LS	CC89589	14 Jan 2011	1667.08	297.72	45.69
H3/H4/H5 LS	CC89589	10 Feb 2012	1666.97	297.63	46.43
H3/CN HS	CC113530	29 Jan 2010	2200.46	358.14	326.22
H3/CN HS	CC113530	12 Jan 2011	2201.21	358.33	327.02
H3 REF	CC73108	1 Feb 2010	1924.41	336.22	199.90
CN LS	CC37840	13 Jan 2011	1684.78	308.85	48.17
CN HS	CC83782	13 Jan 2011	2195.21	356.93	339.56
H4/H5 REF	CC56519	14 Jan 2011	1803.68	331.65	146.47
H4/H5 REF	CC56519	10 Feb 2012	1803.53	331.63	140.47

Evaluation of the Airborne Quantum Cascade Laser Spectrometer (QCLS)

G. W. Santoni et al.

Table 3. Summary of the HIPPO and CalNex flight dates, duration, and locations.

Flight	HIPPO I			HIPPO II			HIPPO III		
	YYMMDD	Hours	Location	YYMMDD	Hours	Location	YYMMDD	Hours	Location
TF01	81213	1.8	CO <> SD	91020	2.5	CO <> OK	100316	2.4	around CO
TF02	81217	4.6	CO <> IO,OK	91022	4.4	CO <> WLEF	100318	3.6	CO <> OK
TF03	90106	1.5	CO <> SD	–	–	–	–	–	–
RF01	90108	1.1	CO -> MT	91031	6.3	CO -> AK	100324	6	CO -> AK
RF02	90109	7.7	MT -> AK	91102	7.3	AK <> NP	100326	8.2	AK <> NP
RF03	90112	6.9	AK <> NP	91104	7.8	AK -> HI	100329	8.4	AK -> HI
RF04	90114	8.4	AK -> HI	91107	8.2	HI -> CI	100331	6.3	HI -> AS
RF05	90116	6.8	HI -> AS	91109	7	CI -> NZ	100402	5.9	AS -> NZ
RF06	90118	6	AS -> NZ	91111	7.7	NZ <> SP	100405	7.8	NZ <> SP
RF07	90120	8.6	NZ <> SP	91114	7.9	NZ -> SI	100408	5.7	NZ -> AS
RF08	90123	7.2	NZ -> TA	91116	8.6	SI -> HI	100410	6.2	AS -> HI
RF09	90126	6.6	TA -> EI	91119	7.7	HI -> AK	100413	8.3	HI -> AK
RF10	90128	7.9	EI -> CR	91121	7.4	AK <> NP	100415	7.8	AK <> NP
RF11	90130	6.1	CR -> CO	91122	4.8	AK -> CO	100416	5	AK -> CO
RF12	–	–	–	–	–	–	–	–	–
RF13	–	–	–	–	–	–	–	–	–
RF14	–	–	–	–	–	–	–	–	–
RF15	–	–	–	–	–	–	–	–	–
RF16	–	–	–	–	–	–	–	–	–
RF17	–	–	–	–	–	–	–	–	–
RF18	–	–	–	–	–	–	–	–	–
Total Flight Hours	81.1			87.6			81.6		
Total Flights	14			13			13		
Flight	HIPPO IV			HIPPO V			CalNex		
	YYMMDD	Hours	Location	YYMMDD	Hours	Location	YYMMDD	Hours	Location
TF01	110607	1.9	CO <> 4cor	–	–	–	100430	5.4	DEN -> ONT
TF02	110609	6.1	CO <> TX	–	–	(see RF02)	–	–	–
TF03	–	–	–	–	–	–	–	–	–
RF01	110614	5.8	CO -> AK	110809	5.1	CO <> WLEF	100504	4.8	SoCAB
RF02	110616	8.9	AK <> NP	110811	6.8	CO <> TX	100507	6.9	SJV
RF03	110618	8.6	AK -> HI	110816	6.1	CO -> AK	100508	7.1	SoCAB
RF04	110622	8.3	HI -> CI	110818	4.2	AK <> NP	100511	7.2	SAC
RF05	110625	6.8	CI -> NZ	110819	8.6	AK <> NP	100512	7.8	SJV
RF06	110628	7.3	NZ -> SP -> HO	110822	7.8	AK -> HI	100514	6.2	SoCAB
RF07	110701	6.8	HO -> DA	110824	8.4	HI -> CI	100516	7.8	SoCAB
RF08	110704	6	DA > SA	110827	7.2	CI -> NZ	100519	6.7	SoCAB
RF09	110706	6.4	SA -> MI	110829	8.9	NZ <> SP	100521	3	SoCAB
RF10	110707	6.2	MI <> AK	110901	6.1	NZ -> CI	100524	6.3	SJV - N
RF11	110710	8.3	AK <> NP	110903	8.6	CI -> HI	100530	5.8	SoCAB - N
RF12	110711	6.5	AK -> CO	110906	8.1	HI -> AK	100531	5.9	SoCAB - N
RF13	–	–	–	110908	8.5	AK <> NP	100602	6.2	SoCAB - N
RF14	–	–	–	110909	4.8	AK -> CO	100603	6.7	SoCAB - N
RF15	–	–	–	–	–	–	100614	7.3	SAC
RF16	–	–	–	–	–	–	100616	6.9	SJV
RF17	–	–	–	–	–	–	100618	7.1	SJV
RF18	–	–	–	–	–	–	100620	7.1	SoCAB
Total Flight Hours	93.9			99.2			122.2		
Total Flights	14			14			19		



Title Page

Abstract Introduction

Conclusions References

Tables Figures

◀ ▶

◀ ▶

Back Close

Full Screen / Esc

Printer-friendly Version

Interactive Discussion

Evaluation of the Airborne Quantum Cascade Laser Spectrometer (QCLS)

G. W. Santoni et al.

Table 4. Biases between QCLS and NWAAS flask measurements at the reported mean concentrations of each species for the five HIPPO campaigns. All test flights and RF01 from HIPPO I are excluded from the analysis.

	CO ₂ bias (ppm)	CO ₂ (ppm)	CH ₄ bias (ppb)	CH ₄ (ppb)	N ₂ O bias (ppb)	N ₂ O (ppb)	CO bias (ppb)	CO (ppb)
HIPPO 1	0.14	385.9	1.2	1788.1	0.61	321.0	−3.71	77.3
HIPPO 2	−0.06	386.7	0.75	1801.2	1.18	320.9	−1.52	84.0
HIPPO 3	−0.09	389.9	0.44	1795.0	1.15	320.0	−1.59	95.3
HIPPO 4	−0.25	390.6	1.04	1800.0	1.23	322.8	−1.14	72.2
HIPPO 5	−0.3	387.5	0.79	1813.7	1.18	322.4	−1.72	74.5
Mean	−0.11		0.85		1.07		−1.94	

Title Page

Abstract

Introduction

Conclusions

References

Tables

Figures

⏪

⏩

◀

▶

Back

Close

Full Screen / Esc

Printer-friendly Version

Interactive Discussion

Evaluation of the Airborne Quantum Cascade Laser Spectrometer (QCLS)

G. W. Santoni et al.

Table 5. Biases between QCLS and Medusa flask measurements at the reported mean concentrations of CO₂ for the five HIPPO campaigns.

	CO ₂ bias (ppm)	CO ₂ (ppm)
HIPPO 1	−0.28	386.16
HIPPO 2	0.03	386.54
HIPPO 3	0.03	389.48
HIPPO 4	−0.14	390.30
HIPPO 5	−0.18	387.70
Mean	−0.11	

[Title Page](#)[Abstract](#)[Introduction](#)[Conclusions](#)[References](#)[Tables](#)[Figures](#)[⏪](#)[⏩](#)[◀](#)[▶](#)[Back](#)[Close](#)[Full Screen / Esc](#)[Printer-friendly Version](#)[Interactive Discussion](#)

Evaluation of the Airborne Quantum Cascade Laser Spectrometer (QCLS)

G. W. Santoni et al.

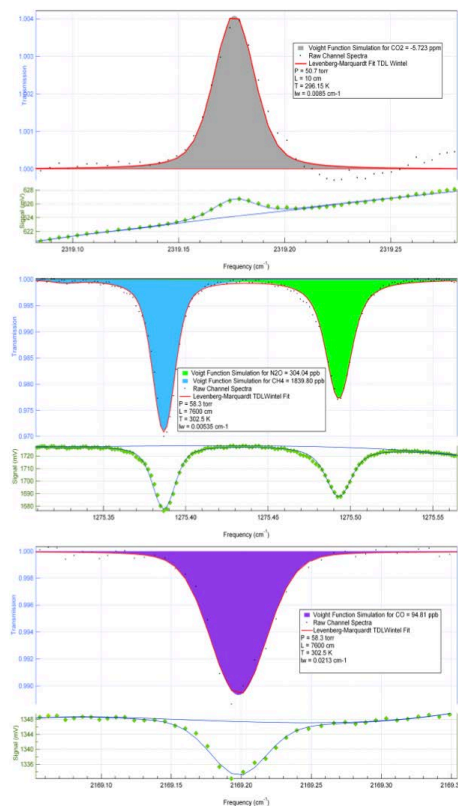


Fig. 1. The absorption spectra for the 3 quantum cascade lasers. QCL1 (a) is a differential measurement of $^{12}\text{CO}_2$ and therefore appears inverted because this sample has a lower concentration of CO_2 than the reference gas. QCL2 (b) shows the spectrum for CH_4 and N_2O and QCL3 (c) shows the spectrum for CO .

Title Page

Abstract

Introduction

Conclusions

References

Tables

Figures

◀

▶

◀

▶

Back

Close

Full Screen / Esc

Printer-friendly Version

Interactive Discussion

Evaluation of the Airborne Quantum Cascade Laser Spectrometer (QCLS)

G. W. Santoni et al.

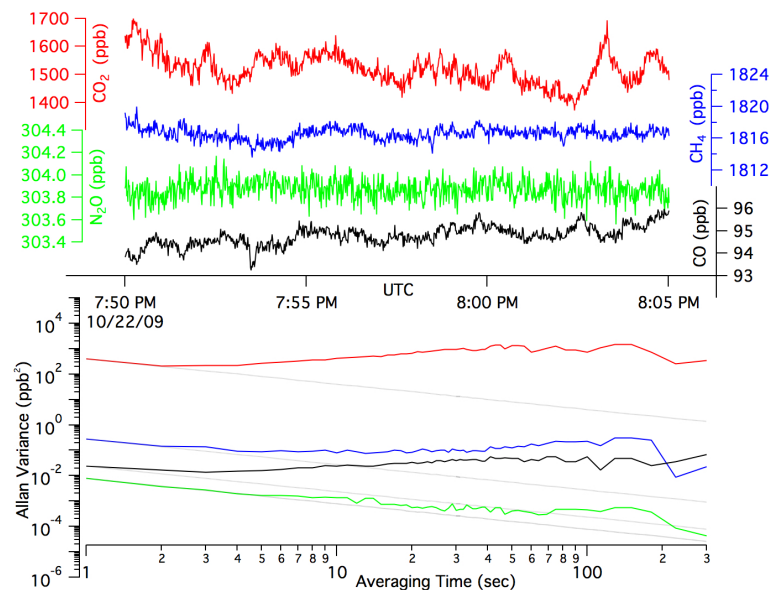


Fig. 2. Time series for the 4 QCLS species during 20 min of in-flight sampling over the Pacific during HIPPO II (top) and the Allan variance as a function of averaging time for the data shown (bottom). Table 1 summarizes these data and also provides corresponding values for sampling from a calibration cylinder in the laboratory. All concentrations are reported in units of ppb, including CO₂, which is the concentration relative to the reference concentration. In this plot, the CO₂ concentration is ~ 1.5 ppm above the reference gas concentrations of ~ 390 ppm.

Evaluation of the Airborne Quantum Cascade Laser Spectrometer (QCLS)

G. W. Santoni et al.

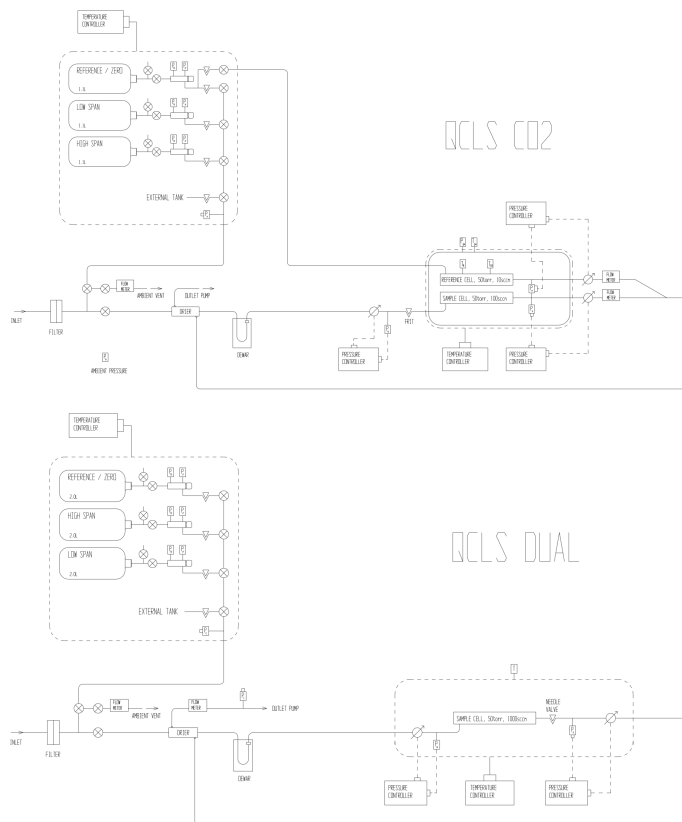


Fig. 3. Schematic of the QCLS-CO2 (top) and QCLS-DUAL (bottom) sampling system.

Title Page

Abstract

Introduction

Conclusions

References

Tables

Figures

◀

▶

◀

▶

Back

Close

Full Screen / Esc

Printer-friendly Version

Interactive Discussion



Evaluation of the Airborne Quantum Cascade Laser Spectrometer (QCLS)

G. W. Santoni et al.

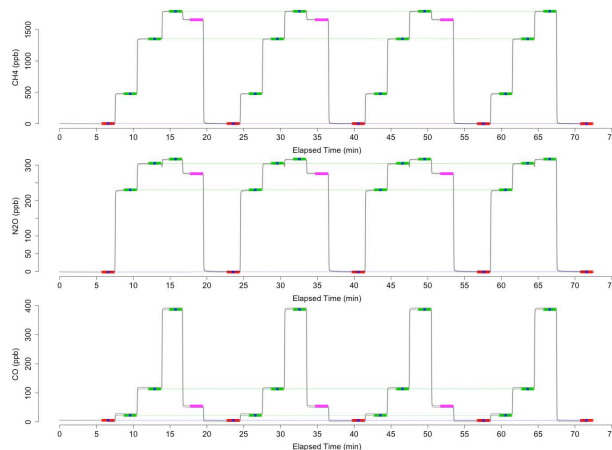


Fig. 4. The sampling sequence used to calibrate a secondary cylinder for QCLS-DUAL (Table 2b) using 3 primary cylinders (Table 2a). Zero air (red) is sampled for 5 min, the primary cylinders are then each sampled for 3 min (green) in order of increasing concentration and then the target secondary cylinder (pink) is sampled for 3 min. We use the last 90 s of a given 5 min zero-air sample (red) to calculate 5 zero-air values. These 5 values are linearly interpolated to the sampling times and that time series (blue trace) is then subtracted from the raw mixing ratios (gray trace). The last 90 s (green) of the “zero-subtracted” data (black trace = gray trace – blue trace) are then averaged to generate a value for each of the 4 primary sampling intervals (blue points). Those 4 values are then linearly interpolated to the QCLS sampling times (green lines). The last 90 s of the target sampling window (pink) are then interpolated to the two primaries that bracket the secondary concentration and that data is shown in Fig. 5.

[Title Page](#)
[Abstract](#)
[Introduction](#)
[Conclusions](#)
[References](#)
[Tables](#)
[Figures](#)
[Back](#)
[Close](#)
[Full Screen / Esc](#)
[Printer-friendly Version](#)
[Interactive Discussion](#)

Evaluation of the Airborne Quantum Cascade Laser Spectrometer (QCLS)

G. W. Santoni et al.

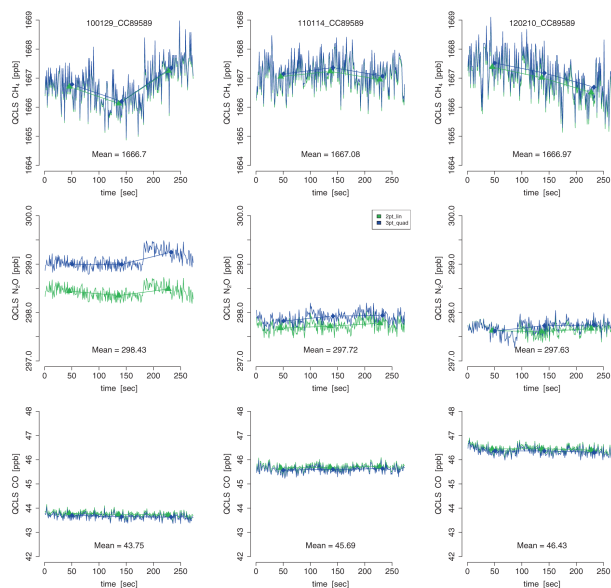


Fig. 5. The concatenated target secondary cylinder interpolated values (i.e. the pink points in Fig. 4) which were linearly interpolated to the bracketing primaries (green) or quadratically interpolated to the three closest primaries (blue). The three columns present the calibration of the secondary cylinder QCLS-DUAL gases CH_4 (top row), N_2O (middle row), and CO (bottom row) for CC89589 on 29 January 2010, 14 January 2011, and 10 February 2012, that was used to fill the gas deck for HIPPO III, IV, and V, illustrating the stability of the tank over time. The values printed on the figure represent the mean of the 270 linearly interpolated values. The standard deviations of these values are roughly 0.4, 0.05, and 0.03 ppb for CH_4 , N_2O , and CO , respectively.

[Title Page](#)
[Abstract](#)
[Introduction](#)
[Conclusions](#)
[References](#)
[Tables](#)
[Figures](#)
[Back](#)
[Close](#)
[Full Screen / Esc](#)
[Printer-friendly Version](#)
[Interactive Discussion](#)

Evaluation of the Airborne Quantum Cascade Laser Spectrometer (QCLS)

G. W. Santoni et al.

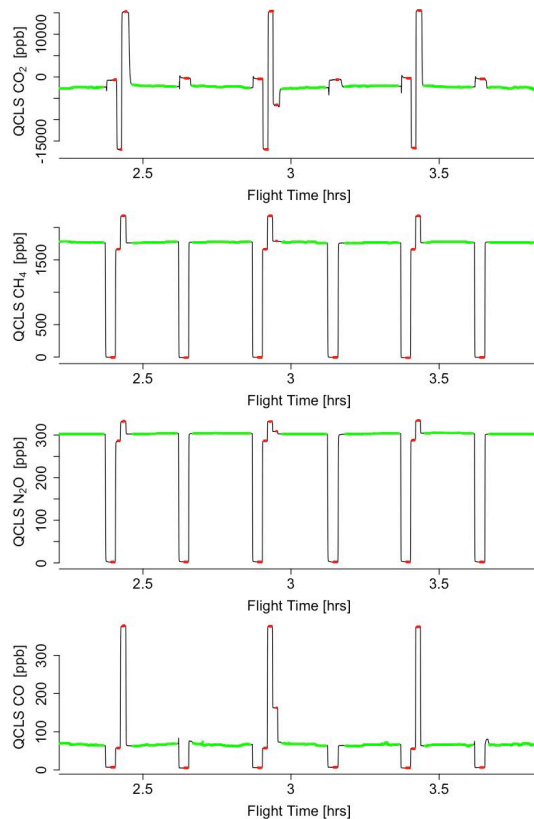


Fig. 6. Calibration sequence of in-flight measurements. The reference gas (QCLS-CO₂) and zero gas (QCLS-DUAL) are sampled every 15 min, a low-span and a high-span every 30 min, and a check-span every two hours. The sample data (green) are then calibrated to the WMO/NOAA scale using the mean values of each group of the calibration spans (red).

[Title Page](#)[Abstract](#)[Introduction](#)[Conclusions](#)[References](#)[Tables](#)[Figures](#)[◀](#)[▶](#)[◀](#)[▶](#)[Back](#)[Close](#)[Full Screen / Esc](#)[Printer-friendly Version](#)[Interactive Discussion](#)

Evaluation of the Airborne Quantum Cascade Laser Spectrometer (QCLS)

G. W. Santoni et al.

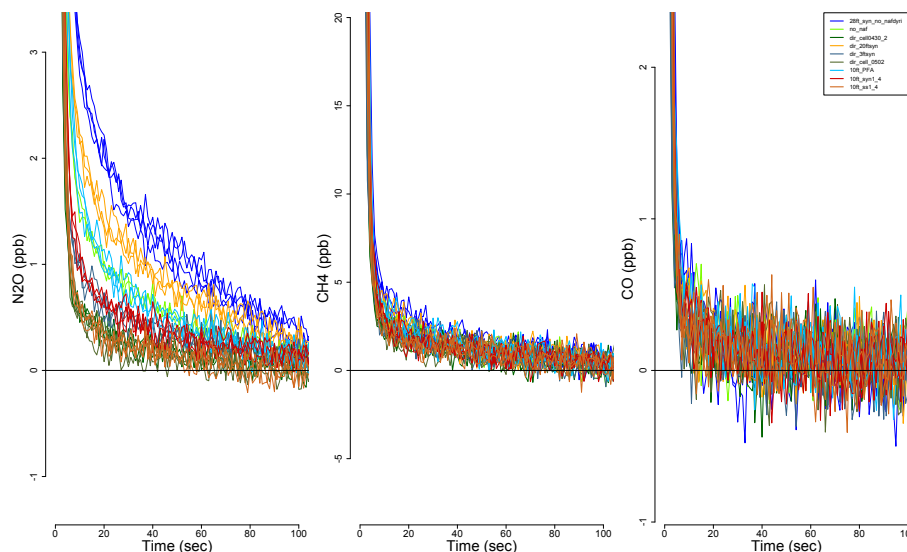


Fig. 7. A series of square-wave tests, alternatively sampling from a check-span secondary tank with ambient concentration and a zero-air tank every 5 min, superimposed upon one another to illustrate the slow sample equilibration time for N_2O . The y axis range is defined as the difference between the dry-air mole-fractions of the secondary tank ($\text{N}_2\text{O} = 319.3$ ppb, $\text{CH}_4 = 1919.6$ ppb, $\text{CO} = 223.4$ ppb) and zero (the zero-air mole-fractions), each divided by 500 to zoom in on the transition region. A decrease in the surface area of PFA or Synflex results in a faster equilibration time. Both CH_4 and CO do not exhibit this behavior.

Evaluation of the Airborne Quantum Cascade Laser Spectrometer (QCLS)

G. W. Santoni et al.

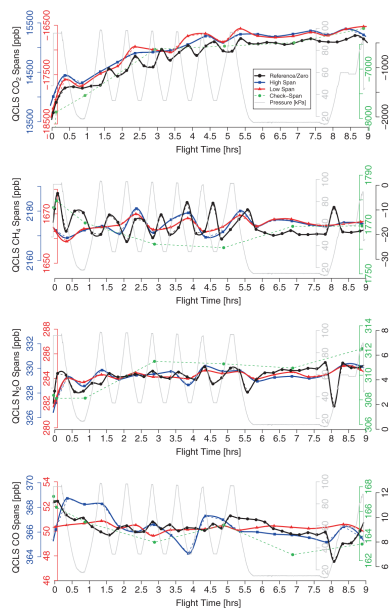


Fig. 8. The gas-deck in-flight calibration addition stability over the course of RF09 on HIPPO V. Each point represents the average of the group of red points in Fig. 6 and the axes for each QCLS species are equivalent in range. The lines represent the Akima spline interpolations to the different spans (red = low-span, blue = high-span, black = zero) and are used to relate the spectroscopically-calibrated mixing ratios to the NOAA scale. QCLS-CO₂ and QCLS-DUAL use different interpolation techniques as discussed in the text. The HIMIL inlet pressure is also shown in gray.

Title Page

Abstract

Introduction

Conclusions

References

Tables

Figures

◀

▶

◀

▶

Back

Close

Full Screen / Esc

Printer-friendly Version

Interactive Discussion

Evaluation of the Airborne Quantum Cascade Laser Spectrometer (QCLS)

G. W. Santoni et al.

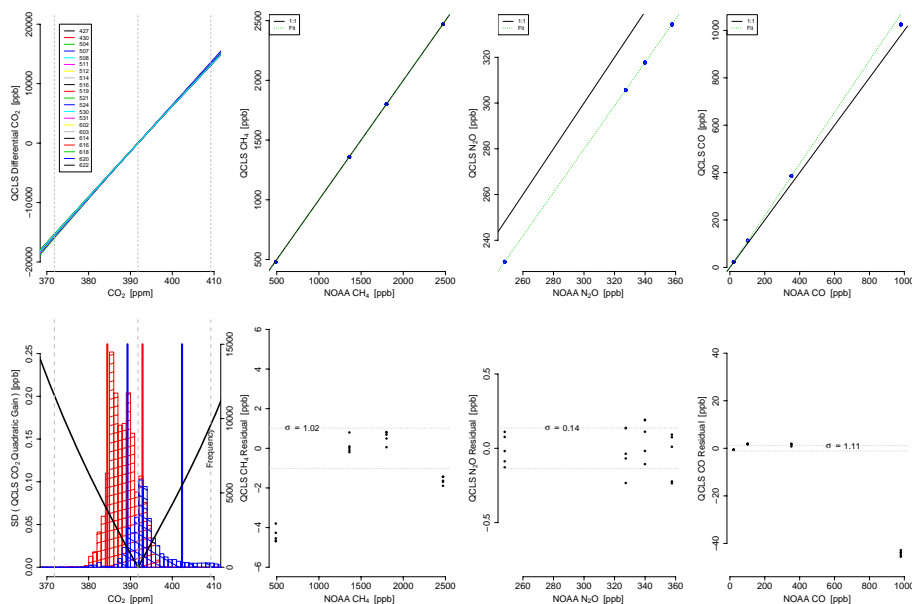


Fig. 9. An estimate of the calibration linearity (top) and uncertainty (bottom) for the 4 QCLS species. For QCLS-CO₂, the quadratic interpolation function for each research flight in CalNex (which was more variable than in HIPPO) is shown. The standard deviation across the 21 flights as a function of calibrated mixing ratio is shown in the bottom panel, reaching a minimum at the value of the reference gas deck calibration cylinder. The histograms of the CalNex (blue) and HIPPO (data) are shown and the 10 % and 90 % quantiles are plotted as vertical lines for each, indicating that the variability in the quadratic interpolation function typically contributes no more than 0.1 ppm. For QCLS-DUAL, the 1 : 1 correspondence of the spectroscopically-calibrated QCLS mixing ratio is plotted against 4 known primary cylinders and regressions are calculated using the error uncertainties from the primary cylinders shown in Table 2a. The bottom plots show the standard deviation of the residual uncertainty, where we exclude the very low CH₄ primary (~ 500 ppb) and the very high CO (~ 1000 ppb) from the uncertainty estimate.

Title Page

Abstract

Introduction

Conclusions

References

Tables

Figures

◀

▶

◀

▶

Back

Close

Full Screen / Esc

Printer-friendly Version

Interactive Discussion

Evaluation of the Airborne Quantum Cascade Laser Spectrometer (QCLS)

G. W. Santoni et al.

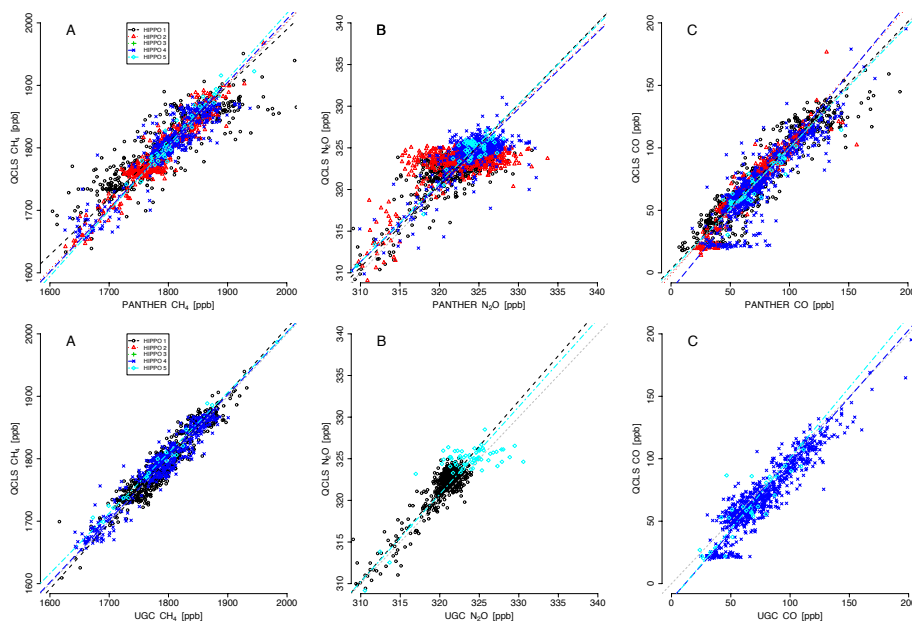


Fig. 11. QCLS-DUAL comparisons to the onboard gas chromatographs PANTHER (top) and UCATS (bottom) for CH_4 (A), N_2O (B), and CO (C). The UCATS instrument had issues with chromatography during HIPPO 2; data are not shown. The HIPPO 4 measurements of N_2O from UCATS were also excluded because of non-linear instrument response during several flights.

[Title Page](#)
[Abstract](#)
[Introduction](#)
[Conclusions](#)
[References](#)
[Tables](#)
[Figures](#)
[◀](#)
[▶](#)
[◀](#)
[▶](#)
[Back](#)
[Close](#)
[Full Screen / Esc](#)
[Printer-friendly Version](#)
[Interactive Discussion](#)

Evaluation of the Airborne Quantum Cascade Laser Spectrometer (QCLS)

G. W. Santoni et al.

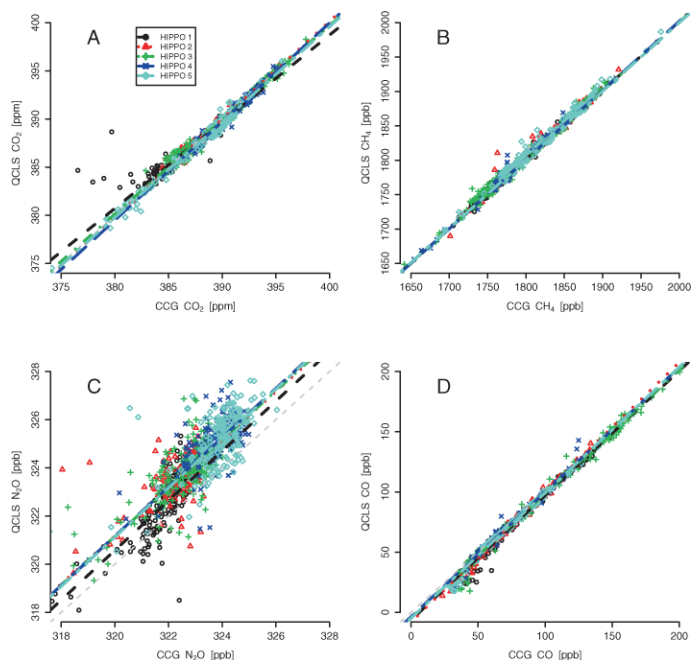


Fig. 12. QCLS comparisons to NOAA flask data during HIPPO I–V for CO₂ (A), CH₄ (B), N₂O (C), and CO (D). With the exception of N₂O which has a much tighter correlation with the flask measurements, the axes are all scaled to the same ranges as Fig. 11. The biases for each fit are reported in Table 4. The type II regressions (York, 2004) in these figures use uncertainty values of 200, 2, 0.2, and 1 ppb for the QCLS measurements of CO₂, CH₄, N₂O, and CO, respectively, corresponding to the calibration uncertainties shown in Table 2a, and half of those values for the NOAA CCG flask values (Zhao and Tans, 2006; Dlugokencky et al., 2005; Hall et al., 2007; Novelli et al., 1994). Test flights were excluded from this analysis. For CO₂, 4 flights during HIPPO-1 were also excluded from the analysis (RF01, RF08, RF10 RF11) as altitude dependent offsets were found and are still under investigation.

Title Page

Abstract

Introduction

Conclusions

References

Tables

Figures

◀

▶

◀

▶

Back

Close

Full Screen / Esc

Printer-friendly Version

Interactive Discussion

Evaluation of the Airborne Quantum Cascade Laser Spectrometer (QCLS)

G. W. Santoni et al.

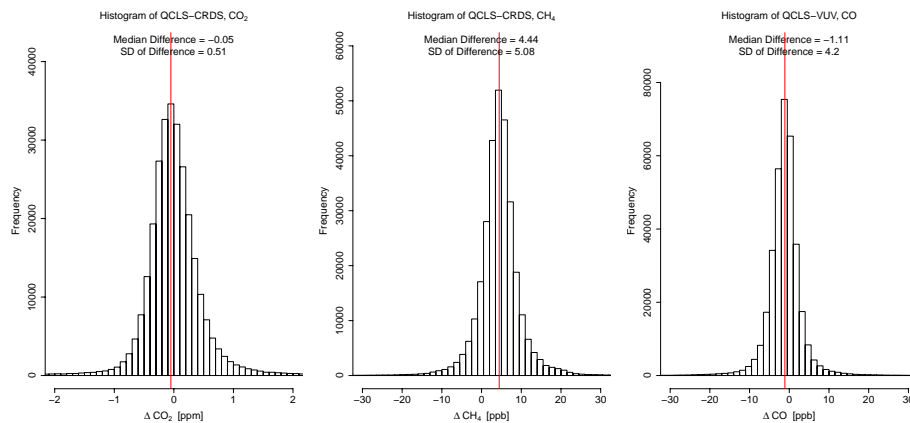


Fig. 13. The 1 Hz CalNex data comparison for QCLS with the NOAA/Picarro CRDS for CO₂ (left) and CH₄ (middle) as well as the comparison with the NOAA VUV sensor for CO (right).

[Title Page](#)[Abstract](#)[Introduction](#)[Conclusions](#)[References](#)[Tables](#)[Figures](#)[⏪](#)[⏩](#)[◀](#)[▶](#)[Back](#)[Close](#)[Full Screen / Esc](#)[Printer-friendly Version](#)[Interactive Discussion](#)